Kinamycins A and C, bacterial metabolites that contain an unusual diazo group, as potential new anticancer agents: antiproliferative and cell cycle effects

Brian B. Hasinoff[a], Xing Wu[a], Jack C. Yalowich[c], Valerie Goodfellow[b], Radoslaw S. Laufer[b], Otunola Adedayo[b] and Gary I. Dmitrienko[b]

The cell growth and cell cycle inhibitory properties of the bacterial metabolites kinamycin A and kinamycin C were investigated in an attempt to determine their mechanism of action and to develop these or their analogs as anticancer agents. Both kinamycin A and kinamycin C have a highly unusual and potentially reactive diazo group. Even with short incubations, both the kinamycins were shown to have very potent cell growth inhibitory effects on either Chinese hamster ovary or K562 cells. Kinamycin C induced a rapid apoptotic response in K562 cells. The cell cycle analysis results in synchronized Chinese hamster ovary cells treated with kinamycin A revealed that they only displayed a G_1/S phase block upon entry to the second cycle. Both kinamycins inhibited the catalytic decatenation activity of DNA topoisomerase IIα, but neither kinamycin acted as a topoisomerase II poison. Their inhibition of catalytic activity was not correlated with cell growth inhibitory effects. Pretreatment of the kinamycins with dithiothreitol protected the topoisomerase IIα activity, which suggested that they may be targeting critical protein sulfhydryl groups, either through reaction with the quinone or with an activated electrophilic diazo group. Neither kinamycin A nor kinamycin C intercalated into DNA, nor were they able to cross-link DNA. Although the cellular target(s) of the kinamycins has yet to be identified, the cluster map analysis, and the cell cycle and proapoptotic effects suggest that kinamycin C has a target different than other established anticancer compounds. *Anti-Cancer Drugs* **17:825–837 © 2006 Lippincott Williams & Wilkins.**

Anti-Cancer Drugs 2006, **17**:825–837

Keywords: anticancer drug, apoptosis, cell cycle, cell cycle block, cytotoxicity, kinamycin, topoisomerase I, topoisomerase II

[a]Faculty of Pharmacy, University of Manitoba, Winnipeg, Manitoba, Canada, [b]Department of Chemistry, University of Waterloo, Waterloo, Ontario, Canada and [c]Department of Pharmacology, University of Pittsburgh School of Medicine, Pittsburgh, Pennsylvania, USA.

Correspondence to B. Hasinoff, Faculty of Pharmacy, University of Manitoba, Winnipeg, Manitoba, R3T 2N2, Canada.
Tel: +1 204 474 8325; fax: +1 204 474 7617;
e-mail: B_Hasinoff@UManitoba.ca

Sponsorship: This work was supported by the Canadian Institutes of Health Research, the Canada Research Chairs Program and a Canada Research Chair in Drug Development for B.B.H., by a grant to J.C.Y. from the NIH (grant CA90787), and by a Discovery Grant to G.I.D. from the Natural Sciences and Engineering Research Council of Canada.

Received 6 March 2006 **Accepted** 19 April 2006

Introduction

Kinamycins A, B, C and D were isolated in 1970 from *Streptomyces murayamaensis*, and were shown to exhibit good activity against Gram-positive but not Gram-negative bacteria [1]. Kinamycin C (Fig. 1) showed a modest increase in survival effect against Ehrlich ascites carcinoma in an animal model [2]. While kinamycin C has been subjected to the 60-cell National Cancer Institute panel, kinamycin A has not. In the 60-cell panel, kinamycin C generally displayed submicromolar GI_{50} values (http://dtp.nci.nih.gov). The kinamycins were initially assigned an *N*-cyanocarbazole structure and it was initially thought that, due to similarities of the indoloquinone system to that of the clinical antitumor agent mitomycin C, the kinamycins likely functioned as reductively activated DNA alkylating agents by a mechanism related to that for the mitomycins [3]. We [4] and another group [5], however, independently determined that the structures assigned to the kinamycins were incorrect, and that the kinamycins are in fact derivatives of diazobenzo[*b*]fluorene, rather than of *N*-cyanobenzo[*b*]carbazole. More recently prekinamycin, a precursor analog of kinamycin, was shown to form a phenyl adduct in the presence of a mild organic reductant and a radical initiator in benzene [6]. Prekinamycin was proposed to undergo a two-step mechanism involving loss of dinitrogen to form a reactive radical intermediate that could damage biological components [6]. The novel antitumor antibiotic lomaiviticin A isolated from a marine actinomycete named *Micromonospora lomaivitiensis* has also recently been found to be extremely potent against a variety of cancer cell lines [7]. The major structural difference between lomaiviticin A and the kinamycin structure is that the former is dimeric, with two kinamycin-like systems joined via a carbon–carbon bond linking ring D of each monomer. In other prior studies, we showed that the diazo group of isoprekinamycin, an analog of kinamycin A, reacted with the nucleophile

0959-4973

Fig. 1

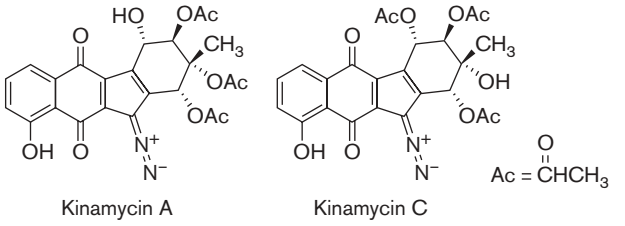

Structures of kinamycin A and kinamycin C.

2-naphthol, which is well known to have good reactivity towards aryldiazonium salts, to yield the azo-coupled product [8]. Collectively, these observations led us to the hypothesis that the kinamycins represent variants of the same pharmacophore in which the diazo group with its diazonium-like character has unusual biological reactivity and plays a key role in their action as cytotoxic agents. Given that the kinamycins are grown in a bacterial growth medium and are isolated with nucleophilic organic solvents, this suggests that they have an attenuated reactivity compared with the reactive organic diazonium compounds. Thus, we were encouraged to investigate the mechanism by which kinamycin A and kinamycin C exert their cell growth inhibitory effects with a view to producing semisynthetic or synthetic analogs with potent anticancer activity. The kinamycins with their diazobenzo[*b*]fluorene pharmacophore are small molecules that are readily amenable to total synthesis and analog development, unlike many other structurally more complex bacterial metabolites. This study is the first to attempt to determine the mechanism by which the kinamycins exert their cytotoxicity towards cancer cells. From the cell cycle and other data we obtained in this study, it is likely that the kinamycins have a potentially new target that is different than the anticancer drugs currently in clinical use.

Methods

Materials

The producing strain, *S. murayamaensis* was obtained from the American Type Culture Collection (Manassas, Virginia, USA), and kinamycin A and kinamycin C were isolated as described [9]. pBR322 plasmid DNA was obtained from MBI Fermentas (Burlington, Ontario, Canada) and the kinetoplast plasmid DNA (kDNA) from TopoGEN (Columbus, Ohio, USA). *Hin*dIII was from Invitrogen (Burlington, Ontario, Canada). Unless indicated, other chemicals were from Sigma (Oakville, Ontario, Canada). The Annexin-V–fluorescein isothiocyanate (FITC) Apoptosis Detection Kit was from Clontech (Palo Alto, California, USA). The 3-(4,5-dimethylthiazol-2-yl)-5-(3-carboxymethoxyphenyl)-2-(4-sulfophenyl)-2H-tetrazolium (MTS) CellTiter 96 AQueous One Solution Cell Proliferation Assay Kit was obtained from Promega (Madison, Wisconsin, USA). Except where indicated, the errors quoted were standard errors from nonlinear least-squares analysis (SigmaPlot, Systat, Point Richmond, California, USA).

Cell culture and growth inhibition assays

Chinese hamster ovary (CHO) cells (type AA8; ATCC CRL-1859), obtained from the American Type Culture Collection, and DZR cells (a dexrazoxane-resistant CHO cell line) [10,11] were grown in α-minimum essential medium (α-MEM; Invitrogen) containing 20 mmol/l 4-(2-hydroxyethyl)piperazine-1-ethanesulfonic acid as described [12]. Human leukemia K562 cells, obtained from the American Type Culture Collection, and K/VP.5 cells (a 26-fold etoposide-resistant K562-derived cell line with decreased levels of topoisomerase IIα protein and mRNA) [13–16] were maintained as suspension cultures in Dulbecco's modified Eagle's medium (Invitrogen) containing 10% fetal calf serum (FCS) and 2 mmol/l L-glutamine. The spectrophotometric 96-well plate cell growth inhibition 3-[4,5-dimethylthiazol-2-yl]-2,5-diphenyl tetrazolium bromide (MTT) (for CHO cells) and MTS (for K562 cells) (Promega, San Luis Obispo, California, USA) assays, which measure the ability of the cells to enzymatically reduce MTT or MTS after treatment with various concentrations of drugs, has been described [12,17]. The drugs were dissolved in dimethylsulfoxide (DMSO). The final concentration of DMSO did not exceed 0.5% (v/v) and was an amount that had no significant effect on cell growth. The cells were incubated with the drugs for the times indicated and then assayed with either MTT or MTS. The 50% inhibitory concentration of drug (IC_{50}) values for growth inhibition in both assays were measured by fitting the absorbance–drug concentration data to a four-parameter logistic equation as described [12].

Topoisomerase IIα kinetoplast plasmid DNA decatenation inhibition assay

A spectrofluorometric decatenation assay was used to determine the inhibition of topoisomerase IIα by kinamycin A and kinamycin C [10,18,19]. kDNA consists of highly catenated networks of circular DNA. Topoisomerase IIα decatenates kDNA in an ATP-dependent reaction to yield individual minicircles of DNA. The 20 µl reaction mixture contained 0.5 mmol/l ATP, 50 mmol/l Tris–HCl (pH 8.0), 120 mmol/l KCl, 10 mmol/l $MgCl_2$, 30 µg/ml bovine serum albumin (BSA), 40 ng kDNA, test compound (0.5 µl in dimethyl sulfoxide) and 10 ng of topoisomerase IIα protein (the amount that gave approximately 80% decatenation). Using a high copy yeast expression vector, full-length human topoisomerase IIα was expressed, extracted and purified as described previously [19]. The final DMSO concentration of 2.5% (v/v) was shown in controls not to affect the activity of topoisomerase IIα. The assay incubation was carried out at 37°C for 20 min and was terminated by the addition of

12 µl of 250 mmol/l Na_2ethylenediaminetetraacetic acid (EDTA). Samples were centrifuged at 8000 *g* at 25°C for 15 min and 20 µl of the supernatant was added to 180 µl of 600-fold diluted PicoGreen dye (Molecular Probes, Eugene, Oregon, USA) in a 96-well plate. The fluorescence, which was proportional to the amount of kDNA, was measured in a Fluostar Galaxy (BMG, Durham, North Carolina, USA) fluorescence plate reader using an excitation wavelength of 485 nm and an emission wavelength of 520 nm.

Escherichia coli DNA gyrase supercoiling inhibition assay

Relaxed plasmid pBR322 DNA used in the gyrase supercoiling assay was prepared by relaxing negatively supercoiled pBR322 DNA with the topoisomerase I present in a K562 nuclear extract (prepared as described in [10]) in the absence of ATP and was purified with a Wizard SV Gel and PCR Clean-up System (Promega). The assay for the inhibition of supercoiling of relaxed pBR322 by gyrase was performed using the Gyrase Assay Kit (TopoGEN). Briefly, 200 µmol/l of either kinamycin A, kinamycin C, a ciprofloxacin-positive control (gift from Anita Vahehaus, Miles, West Haven, Connecticut, USA) or a negative control containing 0.5 µl DMSO was added to 80 ng of relaxed pBR322 DNA in 20 µl of gyrase buffer [35 mmol/l Tris–HCl, pH 7.5, 24 mmol/l KCl, 4 mmol/l $MgCl_2$, 1 mmol/l ATP, 2 mmol/l dithiothreitol (DTT), 1.8 mmol/l spermidine, 6.5% glycerol, 100 µg/ml BSA]. Reactions were initiated by adding 1 unit of *E. coli* DNA gyrase to the reaction mixture for 30 min at 37°C. Reactions were stopped with 3 µl of loading buffer containing 250 mmol/l EDTA, 10 mmol/l Tris–HCl, pH 8.0, 60% w/v sucrose, 0.5% (w/v) bromophenol blue. Supercoiled and relaxed forms of pBR322 were separated by electrophoresis on an agarose gel containing 0.5 µg/ml of ethidium bromide. The fluorescence was visualized using a Alpha Innotech Fluorochem 8900 imaging system (San Leandro, California, USA) equipped with a 365 nm UV illuminator and a CCD camera.

ATP/nicotinamide adenine dinucleotide (reduced form)-coupled ATPase assay

The determination of the ATPase activity of topoisomerase IIα was based on the regeneration of hydrolyzed ATP coupled to the oxidation of nicotinamide adenine dinucleotide (reduced form) (NADH) as described [20]. The ADP produced by the ATPase activity of topoisomerase IIα was rapidly converted back to ATP by pyruvate kinase/phosphoenolpyruvate and the pyruvate produced was converted to lactate by L-lactate dehydrogenase resulting in the oxidation of NADH. The assay measures the rate of loss of the NADH concentration from the absorbance decrease at 340 nm, which is proportional to the steady-state rate of ATP hydrolysis. The assay was performed at 37°C in a 20-µl volume (final concentrations: 50 mmol/l Tris–HCl, pH 8, 120 mmol/l KCl, 10 mmol/l $MgCl_2$, 30 ng/ml BSA, 0.5 mmol/l DTT, 1 mmol/l phosphoenolpyruvate, 20 units/ml pyruvate kinase, 20 units/ml lactate dehydrogenase, 0.5 mmol/l NADH, 75 µmol/l base pair sonicated calf thymus DNA, 1 mmol/l ATP, 25 µmol/l kinamycin C, 500 ng topoisomerase IIα) in a 384-well plate. The absorbance–time data were collected and the initial rates calculated using a Fluostar Galaxy (BMG) microplate reader.

DNA cross-link assay

Kinamycin A and kinamycin C were tested for their ability to cross-link linearized pBR322 DNA as described previously [10]. In this assay, double-stranded linear DNA was heated, which caused the strands to separate. Upon rapid cooling, the strands that were cross-linked by drug treatment recombined to form double-stranded DNA, whereas those that were not cross-linked, did not recombine. Briefly, the pBR322 DNA (1.2 µg) was linearized at a single restriction site with *Hin*dIII restriction enzyme (20 units; Invitrogen) in 20 µl of buffer (50 mmol/l Tris, 1 mmol/l $MgCl_2$, 5 mmol/l NaCl, pH 8.0) and purified by a Wizard SV Gel and PCR Clean-up System (Promega). The 10 µl reaction mixture, which contained linear DNA (100 ng), was incubated with 0.5–50 µmol/l of kinamycin A and kinamycin C for 3 h at 37°C in 10 mmol/l Tris–HCl buffer (pH 6.8). The DNA bifunctional cross-linking agent chlorambucil (50 µmol/l) was used as a positive control. The mixture was then heated at 90°C for 5 min and was then immediately placed in an ice-water bath for 5 min. The double-stranded DNA was then separated by electrophoresis from single-stranded DNA on an ethidium bromide agarose gel (1.2%, w/v). The DNA in the gel was imaged by its fluorescence on a Alpha Innotech Fluorochem 8900 imaging system.

pBR322 DNA relaxation and cleavage assays

Topoisomerase II-cleaved DNA complexes produced by anticancer drugs may be trapped by rapidly denaturing the complexed enzyme with sodium dodecyl sulfate (SDS) [21]. The cleavage of double-stranded closed circular pBR322 DNA to form linear DNA was followed by separating the SDS-treated reaction products using ethidium bromide gel electrophoresis as described [21]. The 20 µl cleavage assay reaction mixture contained 100 ng of topoisomerase IIα protein, 80 ng pBR322 plasmid DNA (MBI Fermentas), 0.5 mmol/l ATP in assay buffer [10 mmol/l Tris–HCl, 50 mmol/l KCl, 50 mmol/l NaCl, 0.1 mmol/l EDTA, 5 mmol/l $MgCl_2$, 2.5% (v/v) glycerol, pH 8.0, and drug (0.5 µl in DMSO)]. The order of addition was assay buffer, DNA, drug and then topoisomerase IIα. The reaction mixture was incubated at 37°C for 10 min and quenched with 1% (v/v) SDS 25 mmol/l Na_2EDTA. The reaction mixture was treated with 0.25 mg/ml proteinase K (Sigma) at 55°C for 30 min to digest the protein. The linear pBR322 DNA cleaved by topoisomerase IIα was separated by electrophoresis

(2 h at 8 V/cm) on a TAE [Tris base (4 mmol/l)/glacial acetic acid (0.11% (v/v))/Na_2EDTA (2 mmol/l) buffer] ethidium bromide (0.5 μg/ml) agarose gel (1.2%, w/v). The DNA in the gel was imaged by its fluorescence on a Alpha Innotech Fluorochem 8900 imaging system.

Topoisomerase I inhibition assay

The topoisomerase I activity present in a K562 nuclear extract (prepared as described previously in [10]) was used to determine whether kinamycin A or kinamycin C inhibited topoisomerase I. Topoisomerase I does not utilize ATP to relax supercoiled DNA. Thus, the 20 μl assay mixture without ATP, and with or without either kinamycin A or kinamycin C, containing 80 ng of pBR322 DNA, 140 ng protein of K562 nuclear extract in the cleavage buffer described above was incubated at 37°C for 10 min, and treated and subjected to ethidium bromide agarose gel electrophoresis as described above to separate the supercoiled DNA from the relaxed DNA.

Cell cycle synchronization and flow cytometry

For the synchronization experiments, CHO cells were grown to confluence in α-MEM supplemented with 10% FCS, 100 units/ml penicillin G, 0.1 mg/ml streptomycin sulfate and 250 ng/ml amphotericin B. Following serum starvation with α-MEM–0.5% FCS for 48 h, the cells were seeded at 3×10^5 cells/ml, repleted with α-MEM–10% FCS and then 5 or 13 h after repletion they were continuously treated with kinamycin A in 35-mm diameter dishes for different periods of time. Cells were fixed with 70% ethanol and stained with a solution containing 20 μg/ml propidium iodide, 100 μg/ml RNase A in 0.1% (v/v) Triton X-100 at room temperature for 30 min. The proportion of cells in sub-G_1, G_0/G_1, S and G_2/M phases of the cell cycle was measured by flow cytometry on a Beckman Coulter EPICS Altra flow cytometer (Beckman Coulter, Mississauga, Ontario, Canada).

The fraction of apoptotic cells induced by treatment of K562 cells with kinamycin C was quantified by two-color flow cytometry by simultaneously measuring integrated green (Annexin-V–FITC) fluorescence and integrated red (propidium iodide) fluorescence. The Annexin-V–FITC binding to phosphatidylserine present on the outer cell membrane was determined using an ApoAlert Annexin-V–FITC apoptosis kit (Clontech). Briefly, K562 cells in suspension were untreated or treated with kinamycin C at 37°C for either 24 or 48 h as indicated. The cells were collected by centrifugation at 700 *g* for 5 min and the pooled cells were washed with the manufacturer-supplied binding buffer. Approximately, 5×10^5 cells were resuspended in 50 μl of manufacturer-supplied binding buffer, and mixed with 1 μl of Annexin-V–FITC at a final concentration of 0.4 μg/ml and 1 μl of propidium iodide at a final concentration of 1 μg/ml. After 30 min of incubation in the dark, the cells were analyzed using flow cytometry.

Thermal denaturation of DNA assay

Compounds that intercalate into DNA stabilize the DNA double-helix and increase the temperature at which the DNA is denatured. The thermal melt temperature (T_m) of sonicated calf thymus DNA (5 μg/ml) was measured in 10 mmol/l Tris–HCl buffer (pH 7.5) in a Cary 1 (Varian, Mississauga, Ontario, Canada) double-beam spectrophotometer by measuring the absorbance increase at 260 nm upon the application of a temperature ramp of 1°C/min. The maximum of the first derivative of the absorbance–temperature curve was used to obtain the T_m. Doxorubicin, which is a strong DNA intercalator, was used as a positive control.

γH2AX assay for DNA double strand breaks in drug-treated K562 cells

K562 cells in growth medium (0.5 ml in a 24-well plate, 1×10^6 cells/ml) were incubated with drug or with DMSO as a control for 5 h. The cells were washed with PBS and lysed with cell lysis buffer containing 30 mmol/l Tris–HCl buffer, pH 7.2, 0.5% Triton X-100, 1/100 protease inhibitor cocktail (1 mmol/l phenylmethanesulfonyl fluoride, 1 mmol/l sodium orthovanadate, 40 mmol/l β-glycerophosphate, 30 mmol/l NaF, 5 mmol/l EDTA). The protein concentration was determined with a Bradford assay. After adding sample buffer [60 mmol/l Tris–HCl, pH 6.8, 10% (v/v) glycerol, 2% (w/v) SDS, 5% (v/v) 2-mercaptoethanol and 0.0025% (w/v) bromophenol blue], the samples were sonicated for 10 s. Cell lysates (15 μg protein) were subjected to SDS–polyacrylamide gel electrophoresis on a 14% gel. Separated proteins were transferred to nitrocellulose membranes, blocked with 5% skimmed milk and incubated overnight with rabbit anti-γH2AX primary antibody diluted 1:2000 (Upstate, Charlottesville, Virginia, USA). This was followed by incubation for 1 h with peroxidase-conjugated goat-anti-rabbit secondary antibody (Sigma) diluted 1:5000. After incubation with ChemiGlow chemiluminescent substrate (Alpha Innotech), chemiluminescence of the γH2AX band was imaged on the Alpha Innotech Fluorochem 8900 imaging system. The glyceraldehyde-3-phosphate dehydrogenase (GAPDH) bands on the blot were likewise imaged after re-probing with mouse monoclonal anti-GAPDH antibody (Stressgen, Victoria, Canada; 1:2000) and peroxidase-conjugated goat anti-mouse secondary antibody (Pierce, Rockford, Illinois, USA; 1:5000).

Self-organizing map-based cluster analysis

The National Cancer Institute has utilized their anti-tumor drug-screening data of more than 100 000 compounds to produce an on-line computational tool (http://spheroid.ncifcrf.gov) utilizing cluster analysis that has led to a self-organizing map (SOM) that clusters 20 000 compounds that share a similar response pattern on the

basis of their cellular activity. These compounds have been placed in six groups designated alphabetically (M, N, P, Q, R and S) with the mnemonics: (M) – mitotic, (N) – membrane integrity, (P) – phosphatase/kinase/cell cycle and (S) – nucleic acid synthesis affecting, with regions Q and R not currently assigned [22]. Kinamycin C was used as a seed in order to determine into which activity cluster it was located.

Results

Kinamycin A- and kinamycin C-induced cell growth inhibition

Both kinamycin A and kinamycin C strongly inhibited cell growth of CHO cells (Fig. 2). Kinamycin A was the more potent of the two compounds and with a 72-h drug treatment the IC_{50} was in the low nanomolar range (Fig. 2). The growth inhibitory effects of both these compounds were strong even with drug exposure times of 1 h or less (Fig. 2). Assuming that the compounds were washed out of the cells, these results suggest that both kinamycin A and kinamycin C acted quickly on their cellular targets to inhibit cell growth.

Fig. 2

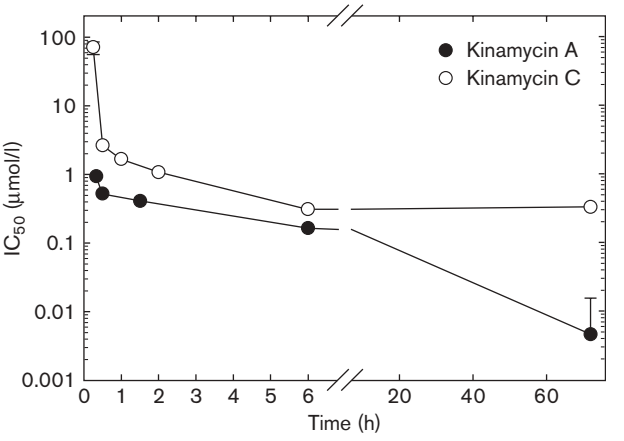

Treatment of Chinese hamster ovary (CHO) cells with kinamycin A (●) and kinamycin C (○) for increasing times strongly decreases their 50% inhibitory concentration of drug (IC_{50}) for growth inhibition. Attached CHO cells were treated for the times indicated with a range of kinamycin A and kinamycin C concentrations. The drugs were then removed by exchanging the medium and the cells were allowed to grow for 72 h. Four-parameter nonlinear least-squares calculated logistic fits of the 3-[4,5-dimethylthiazol-2-yl]-2,5-diphenyl tetrazolium bromide absorbance–kinamycin concentration data were used to obtain the IC_{50} values that are plotted as a function of the time that the cells were exposed to the drugs. Where standard errors are not seen they are smaller than the symbol.

Cell cycle analysis of kinamycin A-treated synchronized Chinese hamster ovary cells and unsynchronized K562 cells

Experiments were carried out on CHO cells synchronized through serum starvation (normal doubling time of 12 h) to determine whether kinamycin A exerted a cell cycle block. The untreated cells were still highly synchronized 5 h after serum repletion as evidenced by the low levels of S and G_2/M phase cells (Fig. 3a and b). The cells went through several complete cell cycles as evidenced by the 12 h periodicity for peaks in the various cell cycle stages (Fig. 3b). Even 53 h after serum repletion, these cells were still well synchronized. As shown in Fig. 3(b), continuous kinamycin A treatment of synchronized cells (beginning 5 h after serum depletion) did not alter progression from G_0/G_1 compared with untreated CHO cells. Kinamycin A-treated cells then entered and passed through their first S phase from 17 to 20 h also nearly normally. The treated cells then passed through their first G_2/M phase with a slight lag compared with untreated cells. These cells fully re-entered G_1 at about 25 h with a lag of about only 4 h compared with untreated cells. Thereafter, they largely remained in G_1 through to the end of the experiment at 53 h, except that after 20 h there was a slow accumulation of S-phase cells. At 53 h, the sub-G_1 apoptotic cells had only reached a level of 4%. These results indicate that kinamycin A induced a G_1/S block, but unusually, only after the cells had traversed one full initial cell cycle.

Experiments were also carried out on synchronized CHO cells that were kinamycin A-treated 13 h after serum repletion in order to determine the effect on cells that had advanced into S phase. By 13 h, 25% of the control cells had entered S phase. The proportion of cells in G_1 and S phases subsequent to kinamycin A treatment closely followed the curves shown in Fig. 3(b). Entry into the first G_2/M phase was delayed by about 4 h as evidenced by the fact that at 17 h the number of cells in G_2/M was small compared with cells treated at 5 h. After 21 h, however, the number of cells in G_2/M closely followed the kinamycin A-treated curve shown in Fig. 3(b). Together, these results indicated that kinamycin A did not act on cell components necessary for exiting G_0/G_1 or entering S phase.

As K562 cells are not readily synchronized by serum starvation, flow cytometry was also carried out on unsynchronized K562 cells (doubling time approximately 24 h) continuously treated with 1 µmol/l kinamycin A. This concentration and that used in the kinamycin C experiments were chosen to obtain approximate equipotency in the degree of cell growth inhibition. At 24 h, the percentage of cells in G_1 was almost unchanged at 43% compared with 48% for untreated cells. The percentage of cells in G_2/M did, however, increase at 24 h to 22% compared with 13% for untreated cells. At 72 h, the cell cycle distribution was similar to that at 24 h, but the percentage of cells in G_1 was decreased slightly to 38% compared with 50% for untreated cells. The percentage of treated cells in G_2/M, which did increase at 72 h to 20% compared with 14% for untreated cells, was likewise

Fig. 3

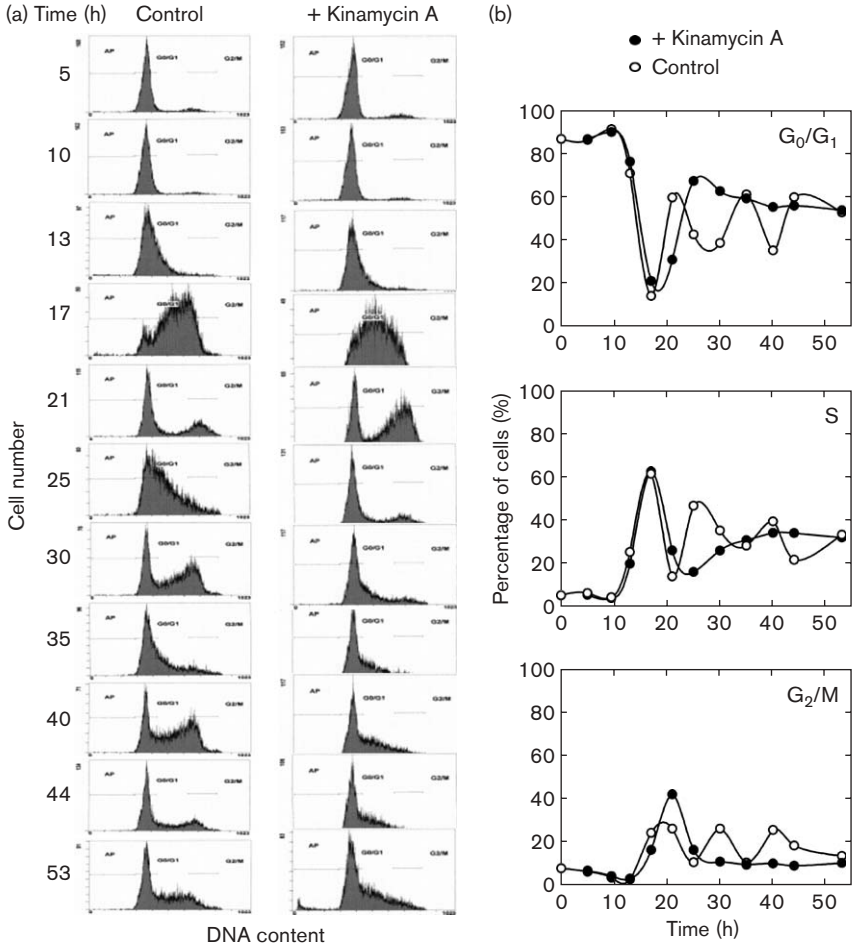

Cell cycle effects of kinamycin A treatment of synchronized Chinese hamster ovary (CHO) cells. CHO cells that had been synchronized in G_0/G_1 through serum starvation were repleted with serum and were untreated (○) or treated (●) with 0.1 μmol/l kinamycin A 5 h after repletion and allowed to grow for the times indicated, after which they were subjected to cell cycle analysis of their propidium iodide-stained DNA. (a) Cell counts are displayed on the vertical axis and the DNA content is plotted on the horizontal axis. (b) Percentage of the cells in G_0/G_1 (top), S (middle) and G_2/M (bottom) phases is plotted as a function of time. The solid lines were a least-squares calculated spline fit to the data. As shown in the top plot, a very high percentage of the cells were initially present in G_0/G_1. After serum repletion, the percentage of control cells in each phase varied periodically as the cells progressed through several cell cycles. The percentage of kinamycin A-treated cells that were present in a sub-G_1 phase was small and only reached a value of about 4% at 53 h.

similar to the percentage at 24 h. Thus, it would appear that kinamycin A did not cause a G_1/S block in K562 cells as they did in synchronized CHO cells (Fig. 3b). Kinamycin A treatment also resulted in about a 2-fold (3.5 compared with 9.5%) increase in the percentage of sub-G_1 apoptotic K562 cells at 72 h.

Cell cycle analysis was also carried out on kinamycin C-treated K562 cells. Treatment of K562 cells with 2 μmol/l kinamycin C resulted in a progressive increase in sub-G_1 apoptotic cells to 15, 27 and 35% at 24, 48 and 72 h, respectively, compared with untreated cells at about 4%. These large percentages of cells in sub-G_1 after kinamycin C treatment made cell cycle comparisons of the remaining cells problematic. As a percentage of cells remaining in the three phases at 24 h, however, kinamycin C treatment moderately decreased the percentage of cells in G_1 to 33% compared with 48% for untreated cells. The percentage of cells in G_2/M was unchanged at 24 h at 15% compared with 13% for untreated cells. At 72 h, the cell cycle distribution was similar to that at 24 h, but the percentage of cells in G_1 was slightly decreased at 39% compared with 50% for untreated cells. The percentage of treated cells in G_2/M was unchanged at 72 h at 15% compared with 14% for untreated cells. The lack of a large cell cycle block in kinamycin A-treated or kinamycin C-treated K562 cells compared with that seen for synchronized CHO cells may have been due to a difference in the two cells or a consequence of synchronization in the case of the CHO cells.

Fig. 4

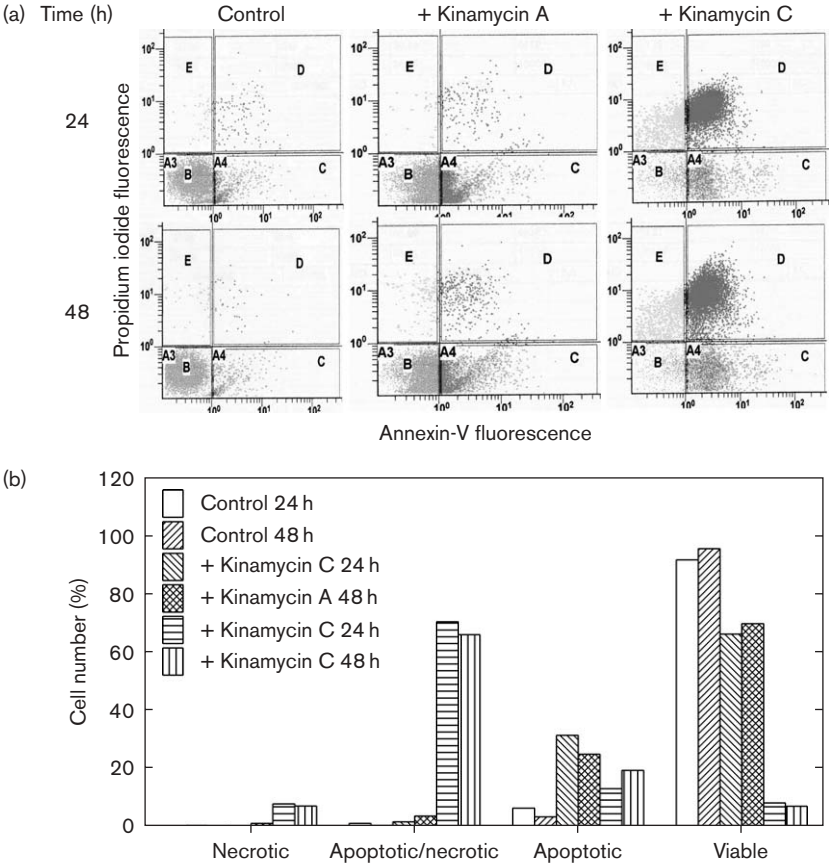

Kinamycin A and kinamycin C treatment of K562 cells induces apoptosis as determined by Annexin-V–fluorescein isothiocyanate (FITC)/propidium iodide two-color fluorescence flow cytometry. (a) Two-color flow cytometry scatter plots of untreated control, kinamycin A (1 μmol/l) and kinamycin C (2 μmol/l)-treated K562 cells for 24 and 48 h, respectively. Annexin-V–FITC binds to the exterior surface of cells that are in the early stages of apoptosis and membrane-impermeant propidium iodide only binds the DNA of necrotic cells that have leaky membranes. Thus, the lower left quadrant contained viable cells; the upper left quadrant contained cells that were necrotic-only; the lower right quadrant contains cells that were apoptotic-only, but were not necrotic; and the upper right quadrant contained cells that were both apoptotic and necrotic. (b) Changes in relative number of cells that were classified as necrotic, apoptotic/necrotic, apoptotic or viable 24 and 48 h after no treatment, or after treatment with either kinamycin A or kinamycin C. At 24 and 48 h after treatment, kinamycin A reduced the proportion of viable cells by about 30% each, and increased the proportion of apoptotic-only cells by 2.2- and 6.8-fold compared with untreated control cells, while the proportion of apoptotic/necrotic cells was almost unaffected. At 24 and 48 h after treatment, kinamycin C reduced the proportion of viable cells by about 90% each, and increased the proportion of apoptotic-only cells by 2.0- and 5.4-fold, compared with untreated control cells, while the proportion of apoptotic/necrotic cells was greatly increased such that they constituted about 65% of the total, compared with control cells each at about 1%. The lettering in the quadrants indicates the gated (letters) and ungated (letters with numbers) areas used in the analysis.

Annexin-V–fluorescein isothiocyanate flow cytometric determination of kinamycin A-induced and kinamycin C-induced apoptosis

Early in the apoptotic process, translocation of the phospholipid phosphatidylserine occurs from the inner to the external plasma membrane of cells. Fluorescent Annexin-V–FITC, which strongly binds phosphatidylserine on cells in the early stage of apoptosis [23], is used to identify apoptotic cells. Thus, Annexin-V–FITC-stained cells in both the lower and upper right quadrants of Fig. 4 are considered to be apoptotic. When used in combination with propidium iodide, which binds DNA, a measure of cells that are necrotic may be obtained as necrotic cell membranes are permeable to propidium iodide. Thus, cells in the lower right quadrant were apoptotic-only and those in the upper right quadrant were apoptotic/necrotic. As shown in Fig. 4, treatment of K562 cells after 24 or 48 h with kinamycin A reduced the proportion of viable cells by about 28%, and increased the proportion of apoptotic-only cells between 4.9- and 7.1-fold compared with untreated control cells, while not substantially changing the proportion of apoptotic/necrotic cells. Kinamycin C, by contrast, greatly reduced the proportion of viable cells (approximately 92%), and greatly increased the proportion of both apoptotic-only cells (2.0- and 5.5-fold) and apoptotic/necrotic cells (57- and 170-fold at 24 and 48 h, respectively) compared with untreated control cells. Thus, as early as 24 h after treatment with

kinamycin C a total of 84% of the cells were apoptotic (sum of apoptotic-only and apoptotic/necrotic cells), which compares to 35% for kinamycin A. While both kinamycin A and kinamycin C were able to induce apoptosis in K562 cells, kinamycin C was clearly much more effective in this regard.

Kinamycin A and kinamycin C inhibit the decatenation activity of topoisomerase IIα

As shown in Fig. 5(a and b), both kinamycin A and kinamycin C inhibited the decatenation activity of human topoisomerase IIα. This assay is a measure of the ability of these compounds to inhibit the catalytic activity only and is not a measure of whether these compounds act as topoisomerase II poisons as do some widely used anticancer drugs [24,25]. Figure 5(a and b) also shows that their inhibitory activity depended upon whether the kinamycins were preincubated with or without 500 μmol/l DTT. In the absence of added DTT, kinamycin A and kinamycin C were about equally potent in inhibiting topoisomerase IIα with IC_{50} values of 7.6 and 9.2 μmol/l, respectively. When either kinamycin A or kinamycin C were, however, preincubated with 500 μmol/l DTT, the IC_{50} value for inhibition increased by 7.5-fold and 11.4-fold, respectively. As can be seen from the CHO cell growth inhibition data in Fig. 2 for a 72-h drug treatment, kinamycin A was far more potent with an IC_{50} value of 4.7 nmol/l compared with the kinamycin C IC_{50} value of 330 nmol/l. The lack of correspondence of the IC_{50} values for topoisomerase IIα inhibition with cell growth inhibition suggests that topoisomerase II was not the target of these drugs.

Inhibition of topoisomerase IIα activity by kinamycin A or kinamycin C was not accompanied by stabilization of the covalent topoisomerase IIα–DNA cleavable complex

Several widely used anticancer agents, including etoposide, are thought to be cytotoxic by virtue of their ability to stabilize a covalent topoisomerase II–DNA intermediate (the cleavable complex) [24,25]. Topoisomerase II alters DNA topology by catalyzing the passing of an intact DNA double-helix through a transient double-stranded break made in a second helix, and is critical for relieving torsional stress that occurs during replication and transcription and for daughter strand separation during mitosis [24,25]. Thus, DNA cleavage assay experiments as described [21] were carried out using etoposide as a control to see whether the test compounds stabilized the cleavable complex. As shown in Fig. 6, the addition of etoposide to the experimental mixture containing topoisomerase IIα and supercoiled pBR322 DNA induced formation of linear pBR322 DNA. Linear DNA was identified by comparison with linear pBR322 DNA produced by action of the restriction enzyme *Hin*dIII acting on a single site on pBR322 DNA. As shown, the addition of up to 250 μmol/l of either kinamycin A or kinamycin C to the reaction mixture, however, induced

Fig. 5

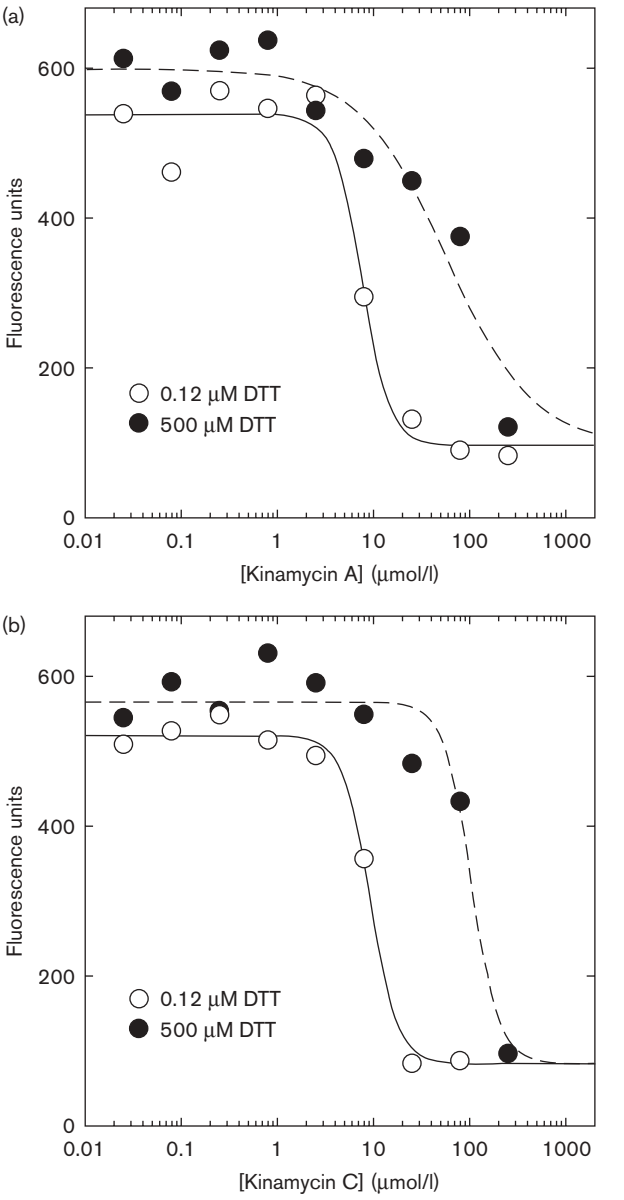

Kinamycin A and kinamycin C inhibit the decatenation activity of topoisomerase IIα. The ability of the compounds to inhibit the topoisomerase IIα-mediated decatenation of highly networked kinetoplast plasmid DNA was measured in an ATP-containing assay mixture at 37°C for 20 min. The fluorescence measures the amount of decatenated DNA minicircles in the supernatant of the centrifuged quenched 20 μl assay mixture. As indicated, the kinamycins were preincubated with or without 500 μmol/l dithiothreitol (DTT) for 1 h at 37°C before adding to the assay mixture. (a) Kinamycin A inhibited the decatenation activity of topoisomerase IIα with 50% inhibitory concentration of drug (IC_{50}) values of 7.6 ± 1.1 and 57 ± 19 μmol/l in the absence and in the presence of added 500 μmol/l DTT, respectively. (b) Kinamycin C inhibited the decatenation activity of topoisomerase IIα with IC_{50} values of 9.2 ± 1.1 and 105 ± 18 μmol/l in the absence (○) and in the presence (●) of added 500 μmol/l DTT, respectively. The solid (no added DTT) and dashed (500 μmol/l DTT) curved lines are nonlinear least-squares calculated fits of the fluorescence–concentration data to a logistic equation. The reaction mixture with no added DTT contained 0.12 μmol/l DTT from the topoisomerase IIα preparation.

Fig. 6

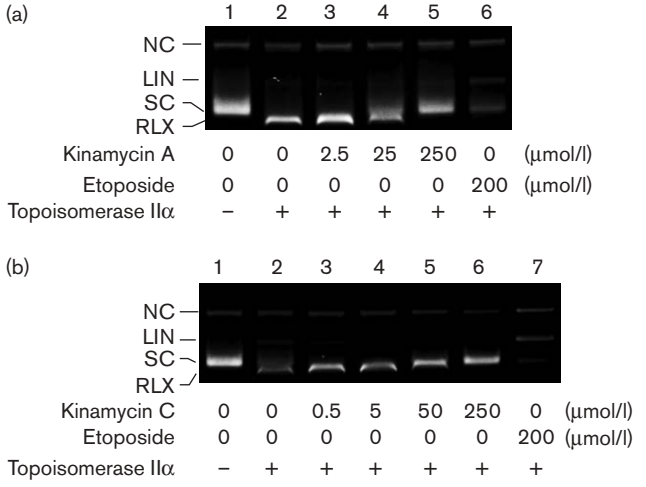

Kinamycin A and kinamycin C inhibit the topoisomerase IIα-mediated relaxation of supercoiled pBR322 DNA, but do not act as topoisomerase IIα poisons to produce linear DNA. (a) This fluorescent image of the ethidium bromide-stained gel shows that topoisomerase IIα relaxed supercoiled pBR322 plasmid DNA (SC) to relaxed DNA (RLX) and that kinamycin A inhibited the relaxation. As shown in lane 2, topoisomerase IIα completely relaxed pBR322 DNA. As shown in lane 6, etoposide treatment produces linear DNA (LIN) and inhibits the relaxation of supercoiled pBR322 DNA. Lanes 3–5 show that the addition of 2.5, 25 or 250 μmol/l kinamycin A progressively inhibited the relaxation of pBR322 DNA. Even at the highest concentration of kinamycin A, only a small amount of linear DNA was produced. A small amount of nicked circular (NC) is normally present in the pBR322 DNA. (b) This gel shows that the addition of kinamycin C to the reaction mixture induced no detectable formation of linear DNA, whereas treatment with etoposide produced a much greater amount of linear DNA (lane 7). Lanes 3–6 show that the addition of 0.5, 5, 50 or 250 μmol/l kinamycin C to the reaction mixture progressively inhibited the relaxation activity of topoisomerase IIα.

little or no detectable formation of cleaved linear pBR322 DNA. The results in Fig. 6 also show that the addition of increasing concentrations of either kinamycin A or kinamycin C to the reaction mixture progressively inhibited the DNA strand passing activity of topoisomerase IIα, as indicated by the progressive loss of relaxed pBR322 DNA relative to supercoiled pBR322. This result is consistent with kinamycin A-induced and kinamycin C-induced inhibition of decatenation when kDNA was the substrate (Fig. 5).

Kinamycin C does not inhibit topoisomerase II by inhibiting its ATPase activity

The ATP concentration at one-half the maximum velocity for the ATPase activity of topoisomerase IIα was measured by varying the ATP concentration from 2 to 1000 μmol/l in the presence and the absence of 25 μmol/l kinamycin C, and fitting the initial ATP hydrolysis rate data to a Michaelis-type saturation equation. In the presence and the absence of 25 μmol/l kinamycin C, the ATP concentrations at one-half the maximum velocity were 62 ± 13 and 58 ± 15 μmol/l, respectively. Thus, it can be concluded that kinamycin C does not inhibit topoisomerase IIα decatenation activity by competing for ATP at the ATP-binding site. For comparison, an ATP concentration at one-half the maximum velocity was determined to be 130 μmol/l for yeast topoisomerase II [20].

The effects of kinamycin A and kinamycin C on the growth of a K562 cell line compared with the K/VP.5 cell line with a decreased level of topoisomerase IIα and on a dexrazoxane-resistant Chinese hamster ovary cell line

One method by which cancer cells increase their resistance to topoisomerase II poisons is by lowering their level or activity of topoisomerase II [14,24]. With less topoisomerase II in the cell, cells produce fewer DNA strand breaks and topoisomerase II poisons are less lethal to cells. These cell lines provide a convenient way to test whether a drug that inhibits topoisomerase II acts as a topoisomerase II poison [19]. Conversely, a lack of change in sensitivity of a putative topoisomerase II poison to a cell line with a lowered topoisomerase II level can be taken to indicate that poisoning of topoisomerase II was not a significant mechanism for this particular agent. We previously showed that the K/VP.5 cell line with acquired resistance to etoposide contained one-fifth the topoisomerase IIα content of the parental K562 cells [13–16]. The IC_{50} for growth inhibition of K562 cells, as measured with the MTS assay, after a 72-h continuous treatment with a range of kinamycin A concentrations, was 0.31 ± 0.03 μmol/l compared with 0.18 ± 0.02 μmol/l for K/VP.5 cells. Thus, because the K/VP.5 cells with the reduced level of topoisomerase IIα were not cross-resistant to kinamycin A, it can be concluded that kinamycin A does not act as a topoisomerase II poison. Similarly, the IC_{50} for kinamycin C treatment of K562 cells was 0.37 ± 0.03 μmol/l compared with 0.17 ± 0.02 μmol/l for K/VP.5 cells. Thus, kinamycin C also did not act as a topoisomerase II poison. These results are consistent with the inability of kinamycin A and kinamycin C to form double-stranded linearized pBR322 DNA in the topoisomerase IIα cleavage assay (Fig. 6).

As kinamycin A and kinamycin C are catalytic inhibitors of topoisomerase IIα, as is the bisdioxopiperazine dexrazoxane [10,11,26], we decided to examine whether the kinamycins might bind to the dexrazoxane-binding site of topoisomerase II [27,28]. Thus, we measured the cross-resistance of our previously characterized dexrazoxane-resistant DZR cell line [10,11,26]. The DZR cell line, which was derived from the parent CHO cell line and has a Thr48Ile mutation in topoisomerase IIα, is highly resistant (400-fold) to dexrazoxane in the MTT assay [10,11,26]. This mutation is located in the N-terminal ATP-binding region of topoisomerase II close to the X-ray-determined dexrazoxane-binding site [27,28].

The IC_{50} for growth inhibition of CHO cells, as measured with the MTT assay after a 72-h continuous treatment with a range of kinamycin A concentrations, was measured to be 0.015 ± 0.007 μmol/l compared with 0.0038 ± 0.0007 μmol/l for DZR cells. Similarly, for kinamycin C IC_{50} values were measured to be 0.087 ± 0.006 μmol/l compared with 0.18 ± 0.03 μmol/l for DZR cells. Thus, because kinamycin A was not cross-resistant and kinamycin C was only slightly cross-resistant (resistance factor of 2.1), we concluded that neither kinamycin inhibited topoisomerase IIα by binding to the dexrazoxane-binding site.

Kinamycin A and kinamycin C do not inhibit topoisomerase I

As some compounds that inhibit topoisomerase II also may inhibit topoisomerase I, it was decided to see whether kinamycin A and kinamycin C, which inhibit topoisomerase IIα, were able to also inhibit topoisomerase I. Using K562 nuclear extract as the source of topoisomerase I in the assay, neither kinamycin A nor kinamycin C at concentrations up to 250 μmol/l were observed to inhibit the topoisomerase I-mediated conversion of supercoiled pBR322 DNA to its relaxed form (data not shown). In a control experiment, camptothecin (8 μmol/l), which is a known topoisomerase I inhibitor [29], completely inhibited relaxation of pBR322 DNA. Thus, it can be concluded that neither kinamycin A nor kinamycin C inhibited cell growth by inhibiting topoisomerase I.

Neither kinamycin A nor kinamycin C increase the thermal denaturation of DNA

Doxorubicin (2 μmol/l), which is a well-known DNA intercalating drug, was used as a control and was observed to increase the T_m of sonicated DNA by 18°C from 70 to 88°C. Neither 5 μmol/l kinamycin A nor up to 25 μmol/l kinamycin C, however, had any measurable effect on the T_m, indicating that at these concentrations they did not intercalate into DNA. Thus, it can be concluded that kinamycin A and kinamycin C did not inhibit cell growth by directly intercalating into DNA.

Kinamycin A and kinamycin C do not cross-link DNA and do not induce DNA double-strand breaks in K562 cells

A temporary cell cycle block by cell cycle checkpoint mechanisms at the G_1/S interface such as that shown in the results of Fig. 3 are characteristic of a cellular response to DNA damage [30]. Thus, in order to determine whether either kinamycin A or kinamycin C damaged DNA, a DNA cross-link assay was performed as well as an examination of H2AX phosphorylation as a surrogate marker assay for DNA double-strand breaks.

When linear double-strand pBR322 DNA was treated with 0.5–50 μmol/l kinamycin A or kinamycin C for 27 h at 37°C, no detectable increase in cross-linked DNA was observed (Fig. 7). Under the same conditions, chlorambucil (50 μmol/l) that was used as a positive cross-linking control agent did produce cross-linked DNA. These results indicated that kinamycin A and kinamycin C did not cross-link DNA, and thus did not inhibit cell growth through their ability to cross-link DNA.

Fig. 7

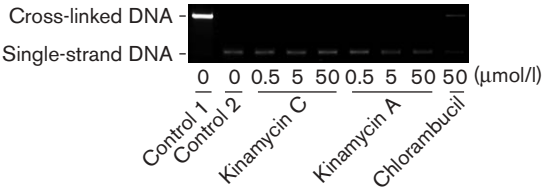

Kinamycin A and kinamycin C do not cross-link linearized pBR322 DNA. This fluorescent image of the ethidium bromide-stained gel shows that the bifunctional alkylating agent chlorambucil control (50 μmol/l) cross-linked DNA while neither kinamycin A nor kinamycin C did. In this experiment, double-stranded linear DNA was incubated with drug or dimethylsulfoxide control for 3 h at 37°C in 10 mmol/l Tris–HCl buffer (pH 6.8). Control 1 was not heated and thus consisted of only double-stranded DNA. Control 2 and the other drug-treated samples were heated to 90°C for 5 min to cause strand separation and then rapidly cooled. The strands that were cross-linked by drug treatment recombined to form double-stranded DNA, whereas those that were not cross-linked, did not recombine. The amount of DNA in each well was the same. The band intensity of the single-stranded DNA is less than that of double-stranded DNA because of reduced binding of ethidium bromide.

Phosphorylated H2AX (γH2AX), which is a variant of an H2A core histone, rapidly localizes at the site of double-strand DNA breaks upon treatment of cells with drugs or ionizing radiation that produce double-strand breaks [31,32]. The thousands of γH2AX molecules that are localized at the site of DNA double-strand breaks are thought to amplify the DNA damage signal and are a widely accepted marker of double-strand breaks [31,32]. Thus, in order to determine whether ether kinamycin A or kinamycin C could induce double-strand breaks in intact K562 cells, the level of γH2AX was determined by Western blotting. As shown in Fig. 8 neither kinamycin A nor kinamycin C detectably increased levels of γH2AX in K562 cells, whereas etoposide, which does produce topoisomerase II-mediated double-strand breaks [21,24], did. Both the DNA cross-link assay and the γH2AX DNA double-strand break assay indicate that these compounds did not damage DNA. These results are in agreement with the lack of kinamycin A and kinamycin C cross-resistance seen in the K/VP.5 cells compared with parental K562 cells, and also with the inability of kinamycin A and kinamycin C to induce formation of linear pBR322 DNA in the topoisomerase II cleavage assay (Fig. 6). These results further confirm that these compounds did not act as topoisomerase II poisons or produce damaging DNA double-strand breaks.

Fig. 8

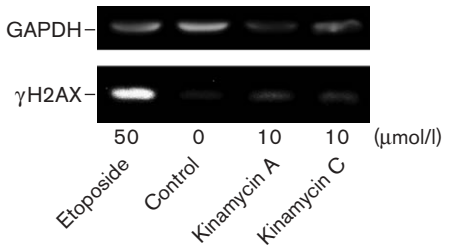

Kinamycin A and kinamycin C do not induce double-strand DNA breaks in K562 cells as indicated by the lack of formation of γH2AX. K562 cells were treated with the concentrations of the drugs indicated for 5 h in growth medium, lysed and subjected to sodium dodecyl sulfate–polyacrylamide gel electrophoresis and Western blotting. The blots were probed with antibodies to γH2AX and glyceraldehyde-3-phosphate dehydrogenase (GAPDH) (as a loading control), and a chemiluminescent secondary antibody. The etoposide positive control, which produces topoisomerase II-mediated DNA double-strand breaks, induced γH2AX formation while neither kinamycin A nor kinamycin C did.

Self-organizing map-based cluster analysis of kinamycin C

When kinamycin C was used as a seed in the National Cancer Institute's antitumor SOM cluster analysis [22] utilizing the complete map, it projected into region Q_3 (cluster k36.9), a region that has not been assigned a function in comparison with some other regions such as region (M) – mitotic, region (S) – nucleic acid synthesis affecting and region (P) – phosphatase/kinase/cell cycle. Thus, this result suggests that kinamycin C exerts its cell growth inhibitory activity on a cellular target different than other anticancer compounds in the SOM.

Discussion

The results of cell cycle analysis on kinamycin A-treated synchronized CHO cells (Fig. 3) showed that they only displayed a G_1/S phase block upon entry to the second cell cycle. While this result is typical of a cellular response to DNA damage [30], the fact that neither the DNA cross-link assay nor the γH2AX DNA double-strand break assay showed any DNA damage indicates that these compounds did not damage DNA through these mechanisms. These experiments, however, do not rule out the possibility that these compounds target DNA as there are many other mechanisms by which small molecules can interact with and damage DNA. The unusual delayed cell cycle block may have occurred because kinamycin A did not directly react with cell components that were necessary for DNA replication and cell division during the first cell cycle. It is possible that the repletion of cells with serum-containing medium before drug treatment allowed for production of all necessary cellular components required for DNA replication in the first cell cycle. Thus, kinamycin A may only have acted on cellular targets required for DNA replication that were newly produced after the first G_2/M phase exit. The reason for the lack of a G_1/S phase block in unsynchronized K562 cells compared with that seen in CHO cells may have been a consequence of the synchronization of the CHO cells or may have been due to differences inherent in the cell types.

It should also be pointed out that kinamycin A and kinamycin C each have three acetate ester groups (Fig. 1), and that these groups may be susceptible to intracellular hydrolysis by esterases to produce over time as many as seven different hydrolyzed deacetylated metabolites of varying activities towards different targets. Thus, a second explanation of the delayed cell cycle effects may be that the active metabolites produced from kinamycin A retained in the cells may not have built up to inhibitory levels until after the completion of the first G_2/M phase. The differing effects of kinamycin A and kinamycin C on induction of apoptosis also suggest that these structurally similar compounds could have different cell targets or may have been differentially activated. The rapid kinamycin C-induced induction of apoptosis in K562 cells is noteworthy as these cells are normally refractory to induction of apoptosis owing to the expression of the product of the Philadelphia chromosome, Bcr–Abl [33,34].

The lack of correspondence of topoisomerase IIα inhibition with cell growth inhibition suggests that topoisomerase II was not the target of the kinamycins. Typically, cells that undergo short treatments with topoisomerase IIα catalytic inhibitors such as dexrazoxane [35] are not strongly growth inhibited because the fraction of cells in the G_2/M phase is relatively small and thus unaffected by inhibition of topoisomerase IIα, which is most highly expressed in this phase [24]. Thus, this result was also consistent with topoisomerase II not being the target of kinamycin A or kinamycin C. Drugs that target topoisomerase II generally display a G_2/M cell cycle block, again because topoisomerase IIα is most highly expressed in this phase [24] and inhibition of its DNA decatenation activity prevents daughter strand separation. The lack of a G_2/M block in either cell line was also consistent with topoisomerase II not being the target of either kinamycin, even though they both are relatively potent inhibitors of topoisomerase IIα *in vitro*. Drugs may also inhibit topoisomerase II by competing for ATP at the ATP-binding site of topoisomerase IIα [24]. Neither kinamycin A nor kinamycin C, however, were able to inhibit the ATPase activity of topoisomerase IIα. The fact that both kinamycin A and kinamycin C inhibited topoisomerase IIα, but were unable to stabilize a covalent topoisomerase IIα-DNA intermediate (the cleavable complex), indicates that neither of these compounds acted as topoisomerase IIα poisons as does etoposide and several other anticancer drugs [24,25]. As neither kinamycin A nor kinamycin C were less active in inhibiting the growth of K/VP.5 cells

with a low level of topoisomerase IIα compared with K562 cells [13–16], it was concluded that neither of these compounds target topoisomerase II.

The fact that the topoisomerase IIα inhibitory activity of both kinamycins depended upon whether they were preincubated with DTT suggested that they may have partially inhibited topoisomerase IIα by binding to critical sulfhydryl groups on the protein. We have shown that topoisomerase IIα is highly sensitive to sulfhydryl-reactive drugs such as quinones [36] and cisplatin [19]. Both these studies showed that topoisomerase IIα can be protected from inhibition by DTT as seen for the kinamycins (Fig. 5). Several other studies have also shown that topoisomerase IIα is sensitive to thiol-reactive agents such as maleimide [37], etoposide orthoquinone [38] and a variety of other quinones, and organic disulfides [39,40]. We also previously showed that in a mass spectrometric proteomics study that at least five cysteine residues (amino acids 170, 216, 300, 392 and 405) on topoisomerase IIα were present mainly as reduced free sulfhydryl groups [19]. Mitomycin A, which is also a quinone, like kinamycin A and kinamycin C, has been shown to undergo reductive activation by DTT and other thiols [41]. Thus, it is possible the normally stable diazo group of the kinamycins becomes activated under the reducing conditions of the cell. It may be that reduction of the quinone makes the diazo group much more electrophilic and it is this process that may be, in part, responsible for the cell growth inhibitory activity of the kinamycins. Whether the specific cellular target of the kinamycins is some critical protein sulfhydryl group (or some other nucleophilic protein group) is not known.

As the SOM cluster analysis suggested that kinamycin C had a target unlike other established anticancer compounds, this indicates the potential importance of these compounds as new anticancer agents. Our previous study [8] showed that isoprekinamycin, a kinamycin analog, formed an adduct with the nucleophile 2-napthol in the presence of Cs_2CO_3 base. This result shows that the kinamycins may be activated to attack by nucleophiles at the diazo group. More recently [6] it was shown that prekinamycin, also a kinamycin analog, under reducing conditions (and in the presence of a radical initiator) formed an adduct with benzene upon loss of dinitrogen. While this latter study was not carried out under cellular conditions, it does suggest that reductive activation to produce highly reactive radical species is a possible mechanism by which the kinamycins exert their cell growth inhibitory activity. Under cellular conditions, reductive activation of the quinone to a semiquinone free radical or to a hydroquinone by either glutathione or reducing enzymes that increases the electrophilic nature of the diazo group, or to directly produce reactive radical species are possible mechanisms by which the kinamycins may exert their potent cell growth activity. Our study was the first to attempt to determine the mechanism by which the kinamycins inhibit the growth of cancer cells. The mechanism by which the kinamycins exert their growth inhibitory effects is the subject of ongoing studies with a view to the development of wholly synthetic analogs as effective anticancer agents.

References

1 Omura S, Nakagawa A, Yamada H, Hata T, Furusaki A, Watanabe T. Structure of kinamycin C, and the structural relation among kinamycin A, B, C, and D. *Chem Pharm Bull* 1971; **19**:2428–2430.

2 Omura S, Nakagawa A, Yamada H, Hata T, Furukawa A, Watanabe T. Structures and biological properties of kinamycin A, B, C, and D. *Chem Pharm Bull* 1973; **21**:931–940.

3 Moore HW. Bioactivation as a model for drug design bioreductive alkylation. *Science* 1977; **197**:527–532.

4 Mithani S, Weeratunga G, Taylor J, Dmitienko GI. The kinamycins are diazofluorenes and not cyanocarbazoles. *J Am Chem Soc* 1994; **116**:2209–2210.

5 Gould SJ, Tamayo N, Melville CR, Cone MC. Revised structures for the kinamycin antibiotics: 5-diazobenzo[*b*]fluorenes rather than benzo[*b*]carbazole cyanamides. *J Am Chem Soc* 1994; **116**:2207–2208.

6 Feldman KS, Eastman KJ. A proposal for the mechanism-of-action of diazoparaquinone natural products. *J Am Chem Soc* 2005; **127**: 15344–15345.

7 He H, Ding WD, Bernan VS, Richardson AD, Ireland CM, Greenstein M, *et al.* Lomaiviticins A and B, potent antitumor antibiotics from *Micromonospora lomaivitiensis*. *J Am Chem Soc* 2001; **123**:5362–5363.

8 Laufer RS, Dmitrienko GI. Diazo group electrophilicity in kinamycins and lomaiviticin A: potential insights into the molecular mechanism of antibacterial and antitumor activity. *J Am Chem Soc* 2002; **124**: 1854–1855.

9 Cone MC, Seaton PJ, Halley KA, Gould SJ. New products related to kinamycin from *Streptomyces murayamaensis*. I. Taxonomy, production, isolation and biological properties. *J Antibiot (Tokyo)* 1989; **42**:179–188.

10 Hasinoff BB, Wu X, Yang Y. Synthesis and characterization of the biological activity of the cisplatin analogs, *cis*-$PtCl_2$(dexrazoxane) and *cis*-$PtCl_2$(levrazoxane), of the topoisomerase II inhibitors dexrazoxane (ICRF-187) and levrazoxane (ICRF-186). *J Inorg Biochem* 2004; **98**:616–624.

11 Hasinoff BB, Kuschak TI, Creighton AM, Fattman CL, Allan WP, Thampatty P, *et al.* Characterization of a Chinese hamster ovary cell line with acquired resistance to the bisdioxopiperazine dexrazoxane (ICRF-187) catalytic inhibitor of topoisomerase II. *Biochem Pharmacol* 1997; **53**:1843–1853.

12 Hasinoff BB, Kozlowska H, Creighton AM, Allan WP, Thampatty P, Yalowich JC. Mitindomide is a catalytic inhibitor of DNA topoisomerase II that acts at the bisdioxopiperazine binding site. *Mol Pharmacol* 1997; **52**:839–845.

13 Ritke MK, Yalowich JC. Altered gene expression in human leukemia K562 cells selected for resistance to etoposide. *Biochem Pharmacol* 1993; **46**:2007–2020.

14 Ritke MK, Allan WP, Fattman C, Gunduz NN, Yalowich JC. Reduced phosphorylation of topoisomerase II in etoposide-resistant human leukemia K562 cells. *Mol Pharmacol* 1994; **46**:58–66.

15 Ritke MK, Roberts D, Allan WP, Raymond J, Bergoltz VV, Yalowich JC. Altered stability of etoposide-induced topoisomerase II–DNA complexes in resistant human leukemia K562 cells. *Br J Cancer* 1994; **69**:687–697.

16 Fattman C, Allan WP, Hasinoff BB, Yalowich JC. Collateral sensitivity to the bisdioxopiperazine dexrazoxane (ICRF-187) in etoposide (VP-16) resistant human leukemia K562 cells. *Biochem Pharmacol* 1996; **52**:635–642.

17 Hasinoff BB, Abram ME, Barnabé N, Khelifa T, Allan WP, Yalowich JC. The catalytic DNA topoisomerase II inhibitor dexrazoxane (ICRF-187) induces differentiation and apoptosis in human leukemia K562 cells. *Mol Pharmacol* 2001; **59**:453–461.

18 Barnabé N, Hasinoff BB. High-throughput fluorescence flow injection topoisomerase II inhibition assay. *J Chromatogr B Biomed Sci Appl* 2001; **760**:263–269.

19 Hasinoff BB, Wu X, Krokhin OV, Ens W, Standing KG, Nitiss JL, *et al.* Biochemical and proteomics approaches to characterize topoisomerase IIα cysteines and DNA as targets responsible for cisplatin-induced inhibition of topoisomerase IIα. *Mol Pharmacol* 2005; **67**:937–947.

20 Lindsley JE, Wang JC. On the coupling between ATP usage and DNA transport by yeast DNA topoisomerase II. *J Biol Chem* 1993; **268**: 8096–9104.

21 Burden DA, Froelich-Ammon SJ, Osheroff N. Topoisomerase II-mediated cleavage of plasmid DNA. *Methods Mol Biol* 2001; **95**:283–289.
22 Rabow AA, Shoemaker RH, Sausville EA, Covell DG. Mining the National Cancer Institute's tumor-screening database: identification of compounds with similar cellular activities. *J Med Chem* 2002; **45**:818–840.
23 Kang YJ, Zhou ZX, Wang GW, Buridi A, Klein JB. Suppression by metallothionein of doxorubicin-induced cardiomyocyte apoptosis through inhibition of p38 mitogen-activated protein kinases. *J Biol Chem* 2000; **275**:13690–13698.
24 Fortune JM, Osheroff N. Topoisomerase II as a target for anticancer drugs: when enzymes stop being nice. *Prog Nucleic Acid Res Mol Biol* 2000; **64**:221–253.
25 Li TK, Liu LF. Tumor cell death induced by topoisomerase-targeting drugs. *Annu Rev Pharmacol Toxicol* 2001; **41**:53–77.
26 Yalowich JC, Thampatty P, Allan WP, Chee G-L, Hasinoff BB. Acquired resistance to ICRF-187 (dexrazoxane) in a CHO cell line is associated with a point mutation in DNA topoisomerase IIα (topo II) and decreased drug-induced DNA-enzyme complexes. *Proc Am Assoc Cancer Res* 1998; **39**:375.
27 Classen S, Olland S, Berger JM. Structure of the topoisomerase II ATPase region and its mechanism of inhibition by the chemotherapeutic agent ICRF-187. *Proc Natl Acad Sci U S A* 2003; **100**:10629–10634.
28 Classen S, Olland S, Berger JM. Structure of the topoisomerase II ATPase region and its mechanism of inhibition by the chemotherapeutic agent ICRF-187. *Proc Natl Acad Sci U S A* 2003; **100**:14510.
29 Sinha BK. Topoisomerase inhibitors. A review of their therapeutic potential in cancer. *Drugs* 1995; **49**:11–19.
30 Friedberg EC. DNA damage and repair. *Nature* 2003; **421**:436–440.
31 Pilch DR, Sedelnikova OA, Redon C, Celeste A, Nussenzweig A, Bonner WM. Characteristics of γ-H2AX foci at DNA double-strand breaks sites. *Biochem Cell Biol* 2003; **81**:123–129.
32 Rogakou EP, Pilch DR, Orr AH, Ivanova VS, Bonner WM. DNA double-stranded breaks induce histone H2AX phosphorylation on serine 139. *J Biol Chem* 1998; **273**:5858–5868.
33 Ritke MK, Rusnak JM, Lazo JS, Allan WP, Dive C, Heer S, *et al.* Differential induction of etoposide-mediated apoptosis in human leukemia HL-60 and K562 cells. *Mol Pharmacol* 1994; **46**:605–611.
34 McGahon A, Bissonnette R, Schmitt M, Cotter KM, Green DR, Cotter TG. BCR-ABL maintains resistance of chronic myelogenous leukemia cells to apoptotic cell death. *Blood* 1994; **83**:1179–1187.
35 Hasinoff BB, Yalowich JC, Ling Y, Buss JL. The effect of dexrazoxane (ICRF-187) on doxorubicin- and daunorubicin-mediated growth inhibition of Chinese hamster ovary cells. *Anticancer Drugs* 1996; **7**:558–567.
36 Hasinoff BB, Wu X, Begleiter A, Guziec L, Guziec F, Giorgianni A, *et al.* Structure–activity study of the interaction of bioreductive benzoquinone alkylating agents with DNA topoisomerase II. *Cancer Chemother Pharmacol* 2006; **57**:221–233.
37 Jensen LH, Renodon-Corniere A, Wessel I, Langer SW, Sokilde B, Carstensen EV, *et al.* Maleimide is a potent inhibitor of topoisomerase II *in vitro* and *in vivo*: a new mode of catalytic inhibition. *Mol Pharmacol* 2002; **61**:1235–1243.
38 Gantchev TG, Hunting DJ. The *ortho*-quinone metabolite of the anticancer drug etoposide (VP-16) is a potent inhibitor of the topoisomerase II/DNA cleavable complex. *Mol Pharmacol* 1998; **53**:422–428.
39 Wang H, Mao Y, Chen AY, Zhou N, LaVoie EJ, Liu LF. Stimulation of topoisomerase II-mediated DNA damage via a mechanism involving protein thiolation. *Biochemistry* 2001; **40**:3316–3323.
40 Lindsey RH Jr, Bromberg KD, Felix CA, Osheroff N. 1,4-Benzoquinone is a topoisomerase II poison. *Biochemistry* 2004; **43**:7563–7574.
41 Paz MM, Tomasz M. Reductive activation of mitomycin A by thiols. *Org Lett* 2001; **3**:2789–2792.